The Nucleus, **44** (3-4) 2007 : 81-90

The Nucleus
A Quarterly Scientific Journal of Pakistan Atomic Energy Commission
NCLEAM, ISSN 0029-5698

REACTIONS INDUCED BY ANTIPROTONS – A REVIEW

*M.A. RANA, M.I. SHAHZAD, S. MANZOOR and G. SHER

Physics Division, PINSTECH, P. O. Nilore, Islamabad, Pakistan

(Received July 10, 2007 and accepted revised form November 27, 2007)

Antiproton interactions with target atoms, its annihilation with a proton or a neutron inside nuclei and decays of excited nuclei formed after antiproton annihilation in them are reviewed here briefly, but comprehensively. Various models describing interactions of antiprotons with matter are examined carefully. Experimental data of antiproton annihilation cross section with nucleons (protons and neutrons), pion emission following annihilation and their interaction with the nucleus, excitation energy of the nucleus and light particle emission for nuclei from ^{12}C to ^{238}U is compiled from the literature and analyzed. Moreover, data sets about antiproton-induced fission of nuclei from ^{209}Bi to ^{238}U and heavy quark pair production are also reviewed. Use of antiprotons for bioapplications is discussed. Results reviewed here make a picture of antiproton annihilation in target nuclei including essential details.

Keywords: Antiprotons, Nuclei, Annihilation, Light particle emission, Fission.

1. Introduction

Antiproton is antiparticle of proton. It has the same mass as proton and charge equal in magnitude but opposite in sign. Antiprotons are a rare component of cosmic radiation and considerable amount of data on $\bar{p}$ flux is available from experiments using balloons. Antiprotons are also produced secondarily in the atmosphere by the interaction of primary cosmic particles with air. These are now produced using high energy accelerators in laboratories like CERN in Switzerland and Fermi Lab. in the United States. In collisions of highly accelerated particles, pairs of particles and antiparticles are produced depending on the energies of colliding particles. For example,

$$p + p \rightarrow p + p + \bar{p} + \bar{p} \qquad (1)$$

Antiproton interactions [1-2] are important as $\bar{p}$ annihilation in nuclei produce very high energy density states in matter. According to Jasterzebski et al. [3], average excitation energy in the case of stopped $\bar{p}$ annihilation in Cu nucleus is similar to average excitation energy achieved by interaction of 2 GeV protons with Cu. Annihilation of antiprotons with one of the nucleons (protons and neutrons) inside nucleus discloses the structure of nucleus due to measurement of antiproton annihilation probabilities with a proton and a neutron inside different nuclei. It is seen for heavier nuclei that probability of annihilation with neutron is greater than the case of light nuclei, which yielded the important conclusion that the ratio of density of neutrons to protons at the surface is greater than N/Z in heavy nuclei [4]. One another good feature of antiproton annihilation is that very hot nuclei with small rotational and compressional energies can be produced using stopped antiproton annihilation [5]. Antiprotons have also been used to study the strangeness and charm [6,7], top-antitop quark [8] and W^+W^- [9] production.

2. Antiproton Annihilation Inside Nucleus

Interaction of a stopped antiproton with matter is complicated than that of a proton. A fast antiproton may annihilate in flight (probability is low) in the target or can be stopped just like a proton losing energy according to Bethe-Bloch formula [10]. A stopped antiproton is captured by the coulomb field of the atom forming an antiprotonic atom. This atom deexcites and antiproton proceeds to lower orbits and finally gets to the nuclear surface where it annihilates with one of the nucleons producing pions. Some of the antiprotons undergo elastic scattering inside the nucleus before they annihilate. According to Ekspong [11], cross section of elastic scattering is one third of the total reaction cross section of antiproton inside the nucleus. The pions formed during annihilation of an antiproton with a nucleon in a nucleus collide with other nucleons. High-energy products of these collisions mostly escape from the nucleus and low energy particles are trapped. This stage of intra nuclear cascade (INC) is very fast (~ 10^{-22} sec)**.** In the next stage (5-10

* Corresponding author : marana@alumni.nus.edu.sg

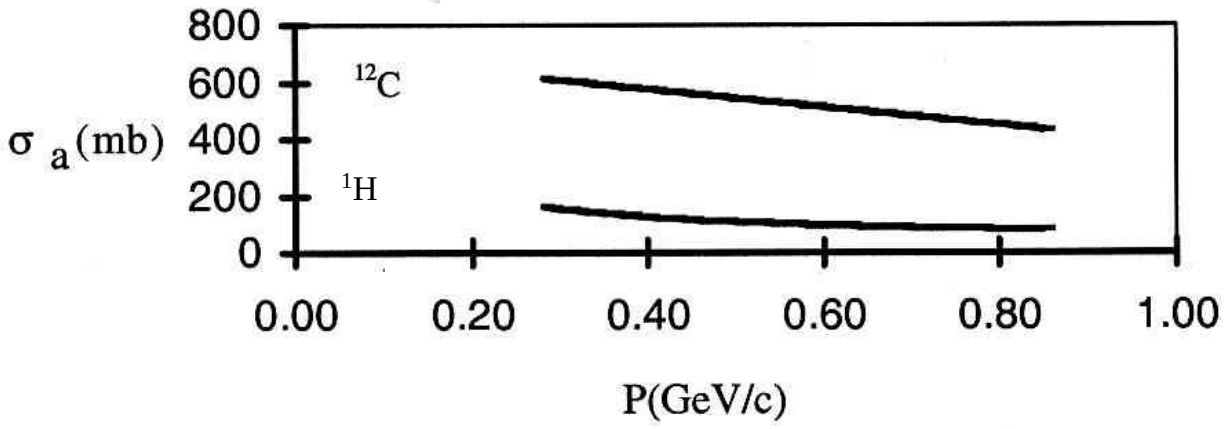

Figure. 1 Antiproton annihilation cross section for ^{1}H and ^{12}C in antiproton momentum range (280-850 MeV).

times 10^{-22} sec), high-energy particles evaporate until the thermodynamical equilibrium is reached. The evaporation cascade continues until the evaporation particles have carried away all the initial excitation energy or nucleus fission takes place [12].

When an $\bar{p}$ annihilates with a free proton or with a nucleon inside the nucleus, pions are generated. The number of pions emitted from an annihilation event lies between 2 and 8. According to Dover and Richard [13], the annihilation forces do not propagate from N to $\bar{N}$, but annihilation potential can only be determined by overlap of N and $\bar{N}$. At high momentum (>1.5 GeV/c), cross section is very low (~50 mb) but increases with the decrease in energy. At low energies, cross section is very high. Dependence of annihilation cross section on antiproton momentum (P) was investigated by Wade et al. [4] and Abrams et al. [14], which resulted in the development of relationships between annihilation cross section and antiproton momentum. These relationships are valid in ~100 MeV/c to ~ GeV/c antiproton momentum range. Relationships for H and C are given below,

$$\sigma_H(P) = 40\,\text{mb} + \frac{34\,\text{mb}}{P}\,(\text{GeV/c}) \qquad (2)$$

$$\sigma_C(P) = 720\,\text{mb} - 317\,P\,\frac{\text{mb}}{\text{GeV/c}} \qquad (3)$$

Graphical representation of equations (2) and (3) is shown in Fig. 1.

The range of antiproton (λ) in homogeneous nuclear matter of density ρ_N =1/7 nucleon/fm^3 is given by the following equation [15],

$$\lambda = \frac{1}{\rho_N \bar{\sigma}_a} = 1.4\,\text{fm}\,[\frac{50}{\bar{\sigma}_a\,[\text{mb}]}] \qquad (4)$$

where $\bar{\sigma}_a$ is the averaged $\bar{p}$ p and $\bar{p}$ n annihilation cross section. At small $\bar{p}$ momentum, (<200 MeV/c), λ is a small fraction of a nucleon diameter. So most of the annihilation reactions occur near the nuclear surface. At higher momentum (>1GeV/c), the size of λ becomes considerable and as a consequence $\bar{p}$ can penetrate deep in the heavy nuclei. According to Rafelski [15], about 2% of annihilations occur at the middle of heavy nuclei for $\bar{p}$ momentum > 1GeV/c. Low and high energy antiprotons can be used as a probe to investigate, respectively, surface and core structure of nuclei. Since the annihilation of low energy antiprotons occurs near the surface in small nuclear matter densities and, consequently, at large distances between nucleons, it is reasonable to assume in this case that annihilation proceeds in vacuum as,

$$\bar{p}p \rightarrow k\pi^- + k\pi^+ + (n_\pi - 2k)\pi^o \qquad (5)$$

$$\bar{p}n \rightarrow k\pi^- + (k-1)\pi^+ + (n_\pi - 2k + 1)\pi^o \qquad (6)$$

Study of antiproton annihilation using cosmic rays has been a hot topic since late fifties. Many authors [16-20] have studied multiplicity and

Table 1. Mean values of multiplicity and energies of charged and total pions produced in $\bar{p}p$ annihilation at rest outside the nucleus [21,22] .

Quantity	$\bar{n}_{\pi^{\pm}}$	$\bar{n}_{\pi}$	Reference
Experiment			
Multiplicity	3.05 ± 0.38	5.01 ± 0.23	[21]
Energy (MeV)	365 ± 17		[22]
Calculation			
Multiplicity	3.04	5.03	[21]

Table 2. Mean values of multiplicities of charged pions produced after absorption of stopped antiprotons on some nuclei from ^{12}C to ^{238}U [21] .

Nucleus	^{12}C	^{70}Ga	^{208}Pb
Experiment	2.72 ± 0.03	2.38 ± 0.11	2.44
Calculation (classical cascade)	2.59 ± 0.08	2.55 ± 0.04	2.46 ± 0.05
Calculation (semi classical cascade)	2.69 ± 0.09	2.55 ± 0.06	2.44 ± 0.05

energies of annihilation pions and strangeness production in detail. Now these reactions can be studied using accelerators. Low energy antiproton ring (LEAR) at CERN has been heavily used by physicists and current facility Antiproton Decelerator (AD) is being used by physics, chemistry and biological studies.

Multiplicity of n_π has narrow peak at $n_\pi = 5$ as clear from Table 1. The kinetic energy of the annihilation pions varies over a wide range from several MeV upto the limit $m_n - m_\pi$. The charges of the pions produced depend on whether the nucleon involved in the annihilation was a proton or a neutron. It can be seen in Table 2 that the multiplicity of pions depends weakly on mass number A of the nucleus involved. Some authors assume that antiproton annihilates with a single nucleon but it may happen with a cluster of nucleons. Formation of high energy and low density quark-gluon plasma which could emit baryons and mesons is possible, especially in case of stopped antiproton annihilation on light nuclei [23] and annihilation of high energy antiprotons (~ 4GeV/c) even on heavy nuclei [24].

3. Interaction of Annihilation Pions with the Nucleus

As five pions are generated per antiproton annihilation on the average, so multi pion nuclear interaction (MPNI) is the most suitable approach to understand the interaction of pions produced with other nucleons inside nucleus. A comparison of calculated mean pion multiplicity with experimental data is given in Table 2. In MPNI, highly excited nuclei with $2m_\pi < E^* < m_N$ are formed which undergo strong spallation ($\Delta A > 20$) and leaving residual nuclei with a large momentum (> 0.7 GeV/c). Probabilities (%) of MPNI with various multiplicities of annihilation pion absorption in case of antiproton annihilation in ^{70}Ga and ^{208}Pb nuclei using classical cascade and quasi- classical models are given in Table 3 [21].

There are two descriptions of MPNI. First is the classical approach. In this picture, the annihilation pions are emitted from point-like sources distributed in space and move further along their classical trajectories. In a nucleus, the incident pions may be scattered elastically or with a charge exchange. In this classical approach, the mean free paths are calculated with low density approximation [25]. For high energy nucleons and pions ($E_\pi > 300\,\text{MeV}$) the classical picture is

Table 3. Probabilities (%) of MPNI with various multiplicities for absorption of antiprotons on ^{70}Ga and ^{208}Pb nuclei using classical cascade model (CCM) and quasi- classical model (QCM)

Multiplicity	^{70}Ga		^{208}Pb	
	CCM	QCM	CCM	QCM
0	17.0	16.4	13.2	9.3
1	24.3	31.7	20.0	29.6
2	27.0	28.3	28.7	32.4
3	19.5	14.8	22.0	18.9
4	9.8	6.3	10.7	7.5
5	2.0	2.0	4.1	2.0
6	0.8	0.5	1.0	0.3
7	--	---	0.2	---
$\overline{\nu}$	1.91	1.71	2.15	1.93

Table 4. Approximate energy range of the particles emitted after annihilation of antiprotons in nuclei from ^{12}C to ^{238}U [22].

Particle	$E_{threshold}$(MeV)	E_{max}(MeV)
P	12.6	227.1
D	16.8	301.7
t	19.8	356.7
^{3}He	44.8	809.0
^{4}He	50.4	905.6

reasonable but not in all situations. So a new model was developed by Iljinov et al. [21] by combining the optical and classical cascade models. They call this model as quasi-classical model.

4. Decay Channels of the Excited Nuclei

4.1. Light particle emission

Antiproton annihilation on a nucleus causes emission of light particles e. g., ^{1}H, ^{2}H, ^{3}H, ^{3}He and ^{4}He nuclei etc. Proton emission takes place by two different processes. One is direct high energy emission with and other is evaporation with low energy. But other particles are mainly emitted directly. It was observed by Hofmann et al. [26] that the ratio of directly emitted protons to evaporated ones increases with the increase of mass number of the target. They have observed the annihilation of stopped antiprotons with the targets from ^{12}C to ^{238}U. For ^{40}Ca, the ratio of high energy to low energy protons, N_{dir} / N_{eva} was 3 and it is close to 18 for ^{238}U. Details of some of the emitted particles [26,27] are given in Tables 4 and 5. Fitted equations (7-10) on the data of 1H, 2H,3H,3He and 4He nuclei emission after annihilation of an antiproton on different nuclei (A=12-238) in Fig. 2 are given below. For protons, deutrons and tritons N is number emitted per antiproton whereas in case of helium ions it is number emitted per 100 antiprotons,

$$N = -3E\text{-}07A^3 + 9E\text{-}05A^2 + 0.0002A + 0.588 \quad (7)$$

$$N = -5E\text{-}08A^3 + 1E\text{-}05A^2 + 0.0002A + 0.0906 \quad (8)$$

$$N=1E\text{-}10A^4 - 6E\text{-}08A^3 + 1E\text{-}05A^2 - 0.0004A + 0.0215 \quad (9)$$

$$N = 2E\text{-}06A^3 - 0.0006A^2 + 0.0495A + 1.1636 \quad (10)$$

$$N= 8E\text{-}07A^3 - 0.0004A^2 + 0.062A + 0.3974 \quad (11)$$

4.2. Fission

We can divide fission into two classes: (i) high energy fission ($E^* \geq 50$ MeV) and (ii) low energy fission ($E^* < 50$ MeV). In most cases, compound nuclei produced after antiproton annihilation are highly excited ($E^* > 100$ MeV). At excitation energy

Table 5. Measured particle yields per antiproton stopped in the target in the given energy interval. Number in first parentheses is the systematic error and second in parentheses is the statistical error. N_{dir}/N_{eva} for protons is also given [26,27].

Nuclide	^{12}C	^{40}Ca	^{63}Cu	^{92}Mo	^{98}Mo	^{238}U
Protons/ $\bar{p}$ $12<E_p<200$ MeV	0.60(4)(1)	0.73(3)(1)	0.86(6)(1)	1.13(4)(1)	1.15(4)(1)	1.23(39)(2)
Deutrons/ $\bar{p}$ $20<E_d<120$ MeV	0.096(6)(3)	0.114(5)(3)	0.152(11)(4)	0.188(8)(5)	0.199(8)(6)	0.229(72)(7)
Tritons/ $\bar{p}$ $25<E_t<60$ MeV	0.018(1)(1)	0.016(1)(1)	0.026(2)(2)	0.027(2)(2)	0.039(2)(3)	0.060(9)(4)
^{3}He/100 $\bar{p}$ $36<E<70$	1.72(4)(13)	2.22(5)(12)	2.60(4)(10)	2.33(5)(11)	2.06(4)(10)	2.66(6)(84)
^{4}He/100 $\bar{p}$ $36<E<70$	1.14(3)(9)	2.18(5)(11)	3.25(7)(26)	3.78(6)(17)	3.69(6)(17)	5.94(9)(190)
^{3}He/^{4}He $36<E<70$	0.66(82)	0.98(3)	1.25(4)	1.63(4)	1.80(9)	2.24(10)
N_{dir}/N_{eva}	5.84(23)(15)	3.01(5)(5)	3.29(3)(7)	3.11(1)(6)	4.70(7)(13)	17.6(5)(10)

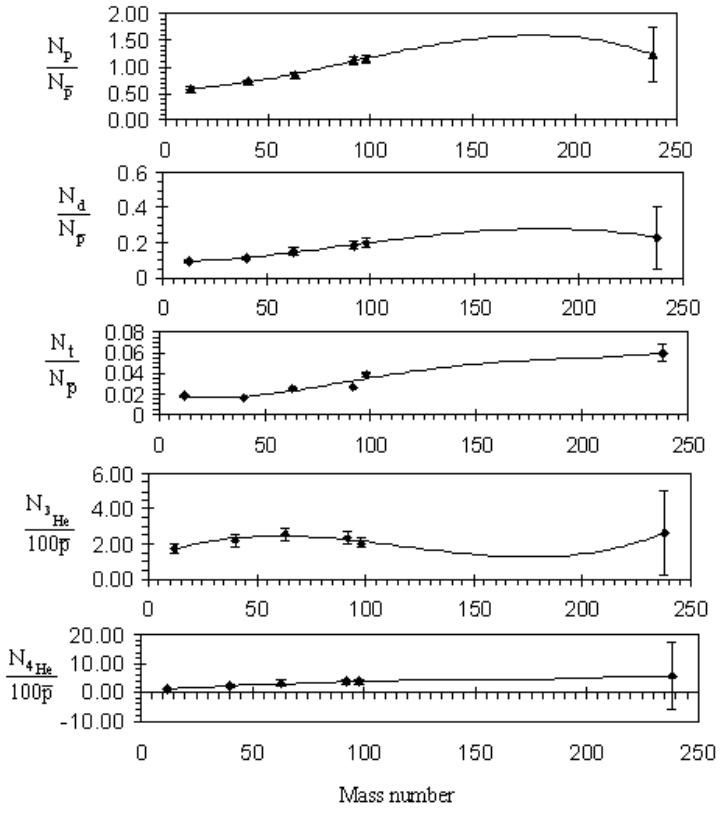

Figure 2. Graphical representation of emitted light particles in the annihilation of antiprotons on different nuclei from ^{12}C to ^{238}U.

(E* ≥ 50 MeV), shell effects disappear and surface of the nucleus is like a liquid drop. Only one fission valley appears on the surface and consequently fission is symmetric. At relatively low excitation energy (E*<50 MeV), two or more fission valleys are formed on the surface of a nucleus due to shell

Table 6. Fission probabilities after antiproton annihilation in heavy nuclei.

Target	Excitation energy(MeV) calculated using [10] and [27]	Fission probability (experimental) [12]	Fission probability (theretical) [12]
^{209}Bi	184 ± 48.70	0.077 (error not given)	0.111 ± 0.003
^{232}Th	216 ± 56.32	0.70 ± 0.04	0.718 ± 0.006
^{238}U	200 ± 52.49	0.77 ± 0.04 (0.84 [27])	0.813 ± 0.006

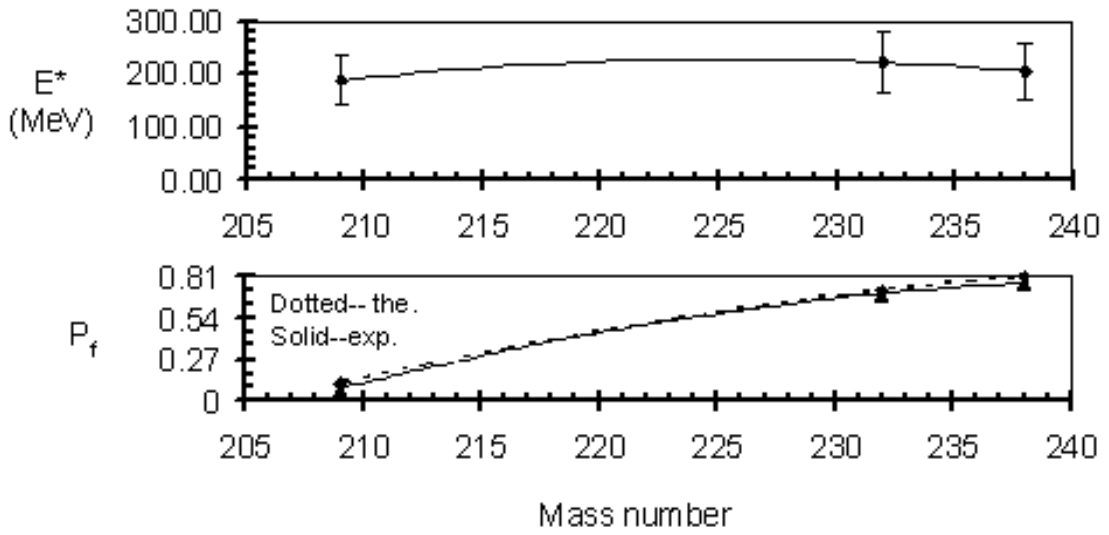

Figure 3. Excitation energy (MeV) and theoretical fission probability of target nuclei after antiproton annihilation for a range of mass number (209-238)

effects. The mode of symmetric fission and one or more modes of asymmetric fission coexist in this case [12]. Only a part of excited nuclei, often after emission of light particles, undergoes fission. Fission probability is high in case of heavy nuclei. In case of ^{238}U, fission probability after antiproton annihilation exceeds 84% [28]. Fission induced by stopped antiprotons is very important because in this case fissioning nucleus have low angular momentum. So we can find the true thermal effects of fission. It should be noted that low angular momentum should have some retardation to fission [27].

Energy and mass distributions of fission fragments are very important. By knowledge of mass distribution of fission fragments, the initial excitation energy of the fissioning nucleus can be determined because the missing mass is a good measure of original excitation energy [29]. Excitation energy per evaporated nucleon is 8 ± 2 MeV [30]. Important features of fission fragments, energy and mass distributions, transient time, and evaporation of particles can de determined by using Langevin Equation [31-33]. Some experimental results of the fission features are given in Table 6 [12,30]. Excitation energy (MeV) and theoretical fission probability Pf as a function of mass number of the target nuclei (209-238) are shown in Fig. 3 and fitted curves are given by equations 12 and 13 respectively,

$$E^* = -0.1434A^2 + 64.678A - 7064 \quad (12)$$

$$P_f = -0.0004A^2 + 0.1869A - 23.058 \quad (13)$$

Many authors (e.g. [5, 27 - 29] have studied mass and charge distributions of fission fragments formed after stopped antiproton annihilations on heavy nuclei. Mass distribution of stopped antiproton induced fission fragments of an important element U^{238} [26] is given in Table 7.

Analysis of the mass distribution is given in Table 8 and shown graphically in Fig. 4. Dependence of total kinetic energy TKE (MeV) of fission fragments on mass number of the target

Table 7. Isotope yield of fission fragments of ^{238}U per 1000 stopped antiprotons [26].

Mass No.	Yield	Mass No.	Yield	Mass No.	Yield
73	4.4 ± 1.3	98	12.2 ± 3.1	116	12.5 ± 2.8
77	3.8 ± 1.3	101	71.9 ± 12.24	117	21.2 ± 3.64
78	7.2 ± 1.71	102	24.4 ± 3.4	120	3.8 ± 1.9
85	9.7 ± 3.1	103	78 ± 50	122	8.4 ± 7.5
87	7.5 ± 2.2	104	25.0 ± 2.2	123	5.6 ± 1.3
88	6.6 ± 1.9	105	76 ± 21.38	125	2.8 ± 0.6
89	12.8 ± 3.4	107	43 ± 9	127	8.4 ± 3.1
90	8.8 ± 2.2	109	10.9 ± 3.4	131	10 ± 4
95	410 ± 310	111	10.6 ± 2.5	132	11.6 ± 2.8
96	10.6 ± 0.9	112	41.4 ± 16.30	141	4.7 ± 1.3
97	229 ± 116.12	115	44 ± 9.85	143	8.8 ± 2.5

Table 8. Isotope yield of fission fragments of ^{238}U per 1000 stopped antiprotons given in above table is divided in 14 classes each of width 5. Average yield of the class is given against mid point of the class.

Mass No.	Yield	Mass No.	Yield
75	4.1 ± 0.92	110	15.725 ± 4.21
80	3.6 ± 0.85	115	15.54 ± 2.17
85	8.6 ± 1.90	120	6.1 ± 3.87
90	9.4 ± 1.49	125	4.9 ± 0.87
95	162.4 ± 82.76	130	10.8 ± 2.44
100	27.125 ± 3.27	140	6.75 ± 1.41
105	44.4 ± 11.03		

nuclei after antiproton annihilation is shown in Fig. 5. The fitted equation on the data in Fig. 5 is,

$$TKE = -0.081A^2 + 35.351A - 3699.8 \quad (14)$$

Important features of fission process of different nuclei after antiproton annihilation and interactions of protons are given in Tables 9 and 10.

4.3. Heavy quark production

Antiprotons can also be used to study the heavy quark production. Hyperons can be produced both by using stopped and inflight antiprotons. In case of stopped antiprotons, antikaons are produced, which causes the

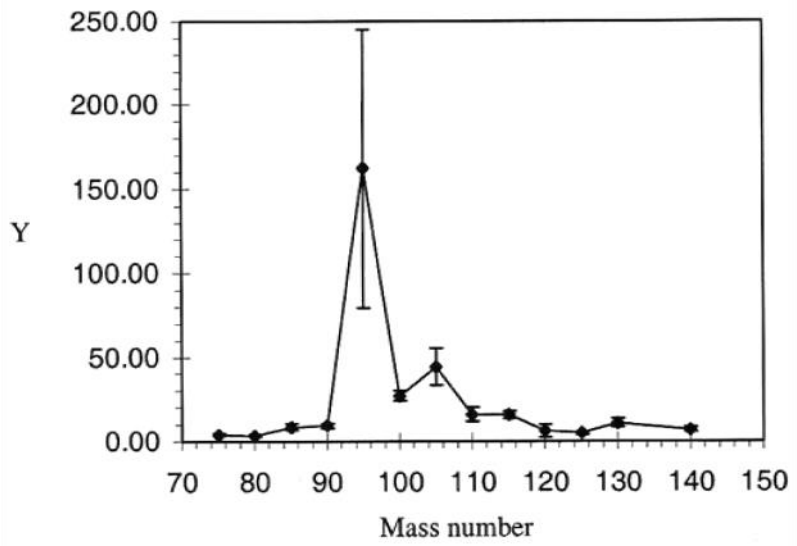

Figure 4. Representation of mass distribution of fission fragments of ^{238}U per 1000 stopped antiprotons given in table 9. Y is the average yield per 1000 stopped antiprotons.

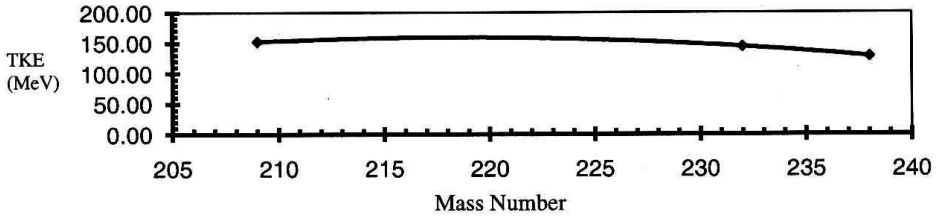

Figure 5. Total kinetic energy (TKE) of fission fragments versus mass number of target nucleus.

production of hyperons [6] as given in Equations 15 and 16,

$$\bar{p} + p \rightarrow \overline{\mathrm{K}} + \mathrm{K} \quad (15)$$

$$\overline{K} + (A-1) \rightarrow \Lambda(\mathrm{A}\text{-}1) + \pi \quad (16)$$

Hyperons can also be produced directly using inflight antiproton annihilation [7]. This is threshold reaction. Quark line diagrams for some of these reactions with energy threshold limits are given in Fig. 6 [34].

5. Conclusions

An antiproton interacts with the target material losing energy like a proton. During its journey in the target material, antiproton is attached with an atom making it an antiprotonic atom. Then, antiproton enters into the nucleus where it annihilates with a proton or a neutron. After annihilation of the antiproton, nucleus is excited with a very high energy up to 2 GeV. This highly excited nucleus decays by emitting high-energy light particles like protons and helium nuclei. Fission of the excited heavy nuclei and formation of heavy quarks also happen under certain conditions. Probability of fission is high in case of heavy nuclei. In flight annihilation of antiprotons produces heavy quarks, which decay further. Study of antiproton interactions with target materials, especially antiproton annihilation in nuclei, are very important as it helps in understanding nucleus structure, meson and baryon interactions, decay modes of ordinary excited nuclei and quark-gluon plasma. Antiproton annihilation in the nuclei has provided significant information about structure of the neutron-rich halo in the nucleus. Low and high energy antiprotons can be used as a probe to investigate, respectively, surface and core structure of nuclei as low energy antiprotons annihilate near surface whereas high energy antiprotons near the core of the nucleus. Antiprotons travel through a tissue (in the same way as in ordinary matter) like protons, but near

Table 9. Different features of fission induced by antiprotons in heavy nuclei [12]

Targets	Average Mass Loss Δm (u)	FWHM of mass loss (u)	FWHM of mass distribution (u)	Average TKE (MeV)	FWHM (TKE) (MeV)
^{238}U	25 ± 2	35.8	44.5	152.2 ± 1.5	38.2
^{232}Th	27 ± 2	28.1	39.1	144.1 ± 1.4	33.1
^{209}Bi	23 ± 2	22.9	38.1	127.9 ± 1.5	30.8

Table 10. Fission probabilities relative to uranium measured for antiproton annihilation at rest and proton with 1GeV and 150 MeV protons.in different targets [30].

Z^2/A of the target	Stopped antiprotons	1 GeV protons	150 MeV protons
31.66	2×10^{-2}	4.3×10^{-2}	-
32.33	4×10^{-2}	1×10^{-1}	3×10^{-2}
33.00	1.1×10^{-1}	1.4×10^{-1}	4.1×10^{-2}

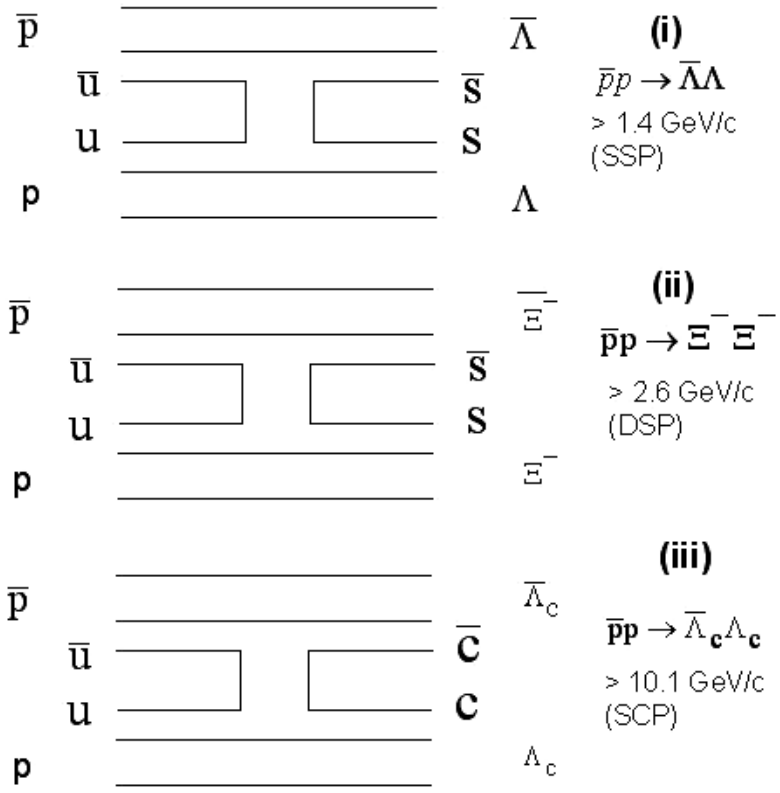

Figure 6. Quark line diagrams for hyperon production with threshold energies

the end of their range they annihilate and deposit excessive energy in the tissue, which makes them suitable for radiotherapy of cancer. So, deeper understanding of antiproton interactions with matter/tissue is beneficial in both physical sciences and perspective bio-applications.

References

[1] K. Sakimoto, Phys. Rev., A **74** (2006) 022709.

[2] G. Andersen et al., Phys. Rev. Lett., **98** (2007) 023402

[3] J. Jastrzebski, W. Kurcewicz, P. Lubinski, A. Grabowska, A. Stolarz, H. Daniel, T. von Egidy, F. J. Hartmann, P. Hofmann, Y. S. Kim, A. S. Botvina, Ye. S. Golubeva, A. S. Iljinov, G. Riepe and H. S. Plendl, Phys. Rev., C **47** (1993) 216.

[4] M. Wade and V. G. Lind, Phys. Rev., D **14** (1976) 1182.

[5] D. Polster, D. Hilscher, H. Rossner, T. von. Egidy, F. J. Hartmann, J. Hofmann, W. Schmid, I. A. Pshenichnov, A. S. Iljinov, Ye. S. Golubeva, H. Machner and H. S. Plendl, Phys. Rev. C **51** (1995)1167; J. Cugnon, P. Deneye and J. Vandermeulen, Nucl. Phys. A. **513** (1990) 636 ; P. D. Barnes et al., Phys. Rev. C **54** (1996)2831; S. Abachi et al., Phys. Rev. Lett. **76** (1996) 2222; F. Abe et al., Phys. Rev. Lett., **78** (1997) 4536.

[6] T. Von Egidy, Nature, **328** (1987) 773.

[7] A. G. Ekspong, Ark. F. Fysik, **16** (1959) 129.

[8] P. Hofmann, A. S. Iljinov, M. V. Mebel, H. Daniel, P. David, T. von Egidy, T. Haninger, F. J. Hartmann, J. Jastrzebski, W. Kurcewicz, J. Lieb, H. S. Plendl, G. Riepe, B. Wright, and K. Ziock, Phys. Rev. C **49** (1994) 2555.

[9] Carl B. Dover and J. M. Richard, Phy. Rev. C **21** (1982) 1466.

[10] R. J. Abrams, R. L. Cool and G. Giacomelli, Phys. Rev. D **4** (1971) 3235.

[11] J. Rafelski, Phys. Lett., B **91** (1980) 281.

[12] N. Horwitz, D. Miller, J. Murray and R. Tripp, Phys. Rev. **115** (1959) 472.

[13] L. Agnew, Jr., T. Elioff, W. B. Fowler, R. L. Lander, W. M. Powell, E. Serge, H. M. Steiner, H. S. White, C. Wiegand and T. Ypsilantis , Phy. Rev. **118** (1960) 1371.

[14] O. Chamberlain, G. Goldhaber, L. Jauneau, T. Kalogeropulos, E. Serge and R. Silberberg, Phy. Rev. **113** (1959) 1615.

[15] W. H. Barkas, R. W. Birge, W. W. Chupp, A. G. Ekspong, G. Goldhaber, H. Heckman, D.H. Pirkins, J. Sandweiss, E. Serge, F. M. Smith, D. H. Stork, L. van Rossum, E. Amaldi, G. Baroni, C. Castagnoli, C. Franzinetti and A. Manfredini, Phys Rev. **105** (1957) 1037.

[16] A. Berthelot, C. Choquet, A. Daudin, O. Goussu and F. Levy, Nucl. Phys. **14** (1960) 545.

[17] A.S. Iljinov, V.I. Nazarkuk and S. E. Chigrinov, Nucl. Phys. A, **382** (1982) 378.

[18] A. G. Ekspong, A. Frisk, S. Nilsson and B. E. Ronne, Nucl. Phys., **22** (1961) 353.

[19] S.C. Phatak and N. Sarma, Phys. Rev. C, **36** (1987) 864.

[20] J. Rafelski, Phys. Lett. B**207** (1988) 371.

[21] V. S. Barashenkov et al., Usp. Fiz. Nauk **109** (1973) 91.

[22] P. Hofmann, F. J. Hartmann, H. Daniel, T. Von Egidy, W. Kanert, W. Markiel, H. S. Plendl, H. Machner, G. Riepe, D. Protic, K. Ziock, R. Marshall and J. J. Reidy, Nucl. Phys. A**512** (1990) 669.

[23] W. Markiel, H. Daniel, T. von Egidy, F. J. Hartmann, P. Hofmann, W. Kanert, H. S. Plendl, K. Ziock, R. Marshall, H. H. Machner, G. Riepe and J.J. Reidy, Nucl. Phys. A**485** (1988) 445.

[24] H. Machner, Sa Jun, G. Riepe, D. Protic, H. Daniel, T. von Egidy, F. J. Hartmann, W. Kanert, W. Markiel, H. S. Plendl, K. Ziock, R. Marshall, and J. J. Reidy, Z. Phys A-Hadrons and Nuclei **343** (1992)7 3.

[25] Y. S. Kim, A. S. Iljinov, M. V. Mebel, P. Hofmann, H. Daniel, T. von Egidy, T. Hainger, F. J. Hartmann, H. Machner, H. S. Plendl and G. Riepe, Phys. Rev. C **54** (1996) 2469.

[26] J.P. Bocquet, F. Malek, H. Nifenecker, M. Rey-Campagnolle, M. Maurel, E. Monnand, Perrin, C. Ristori, G. Ericsson, T. Johansson, G. Tibell, S. Polikanov, T. Krogulski and J. Mougey, Z. Phys. A-Hadrons and Nuclei **342** (1992) 183.

[27] T. Wada, N. Carjan and A.B.E. Yasuhisa, Nucl. Phys. A **538** (1992) 283c.

[28] I.I. Gonchar, G. I. Kosenko, N. I. Pischasov, and O. I. Serdyuk, Sov. J. Nucl. Phys. **55** (1992) 514.

[29] Gonchar and P. Frobrick, Nucl. Phys. A **551** (1993) 495.

[30] R. A. Eisenstein, Nucl. Phys. A **558** (1993) 569c.